JOURNAL OF MATERIALS SCIENCE 32 (1997) 2759–2769

Crack formation in mesophase pitch-based carbon fibres

Part II *Detailed structure of pitch-based carbon fibres with some types of open cracks*

SEONG-HO YOON, YOZO KORAI, ISAO MOCHIDA
Institute of Advanced Materials Study, Kyushu University, Kasuga, Fukuoka, 816, Japan

Several mesophase pitch-based carbon fibres showing radial textures in their transverse alignments were observed by high resolution scanning electron microscope (HR-SEM) to elucidate the principal factor that induces the open crack in the transverse sections of the fibre along its fibre axis. The HR-SEM images of transverse sections exhibited various features in the alignment and shapes of the domains, although they were approximately arranged in the radial direction. The alignment of the domains was often variable in the locations from the outer part to the centre. Linear domains radially oriented in the outer part of the transverse section, that induce the circumferential shrinkage at the spinning and further heat-treatment steps, were essential for the development of open cracks with the PAC-man shaped fibre. Non-radial alignment or non-linear, bent or loop domains in the outer parts prohibited the development of the crack; these are observed in the fibres with the radial skin–random core and the onion skin–radial core alignments. Fibres without cracks in their as-spun or stabilized states usually showed shallow cracks even after the graphitization because the bent and loop domains in the intermediate and centre parts prohibited cracks from propagating into the centre part because the graphitic shrinkage along the domain shapes cannot be linear.

1. Introduction

Open wedge cracking, often observed in high performance mesophase pitch-based carbon fibres, has been recognized as one of the key mechanisms in the deterioration of their mechanical properties [1]. The radial alignment in the transverse section of the carbon fibre has been believed to originate the crack [2] and the spinning conditions such as spinning temperature [3, 4], melt viscosity and nozzle dimensions [5], and the nature of mesophase pitch [6] are very influential on the development of such an alignment. However, the cracks are found by optical microscopy to exhibit various depths and angles in the radial texture suggesting a dependence on the more detailed structure in the transverse section of the mesophase pitch-based carbon fibre [7].

There have been some papers which described the transverse microtexture of the pitch-based carbon fibres by transmission electron microscopy. Lafdi *et al.* [8] reported that the transverse radial alignment in the anisotropic pitch-based carbon fibres originates from the micelle edge-to-edge network, defining the texture with a wedge. Taylor and co-workers [9, 10] have reported that Amoco fibres are made of two types of structurally distinct domains, either microporous or dense. They also claimed that the strength of the fibres influenced the transverse microstructural features such as the nature of the domains, their size, shape, and distribution. A folded domain structure with no microporosity was speculated to improve the strength of Du Pont fibre. Endo [11] also reported that his mesophase pitch-based carbon fibres carrying a less-graphitic, and folded microstructure were stronger than Amoco fibres of more sheet-like graphitic and planar structure.

Recently, the present authors reported, using high resolution scanning electron microscopy (HR-SEM), that the carbon fibre is believed to be composed of domain units which are composed of several or tens of micro-domains gathering to form linear, bent, and loop domain shapes in the mesophase pitch-based carbon fibres with various transverse textures [12]. Such domains are arranged in various combinations and manners to form more complex alignments in both the transverse and longitudinal sections of the carbon fibre than those expected to be observed by an optical microscope of lower resolution. Such an SEM observation has the advantage of giving a much broader feature of the carbon fibre.

All such reports indicate that the changes in the shapes and properties of the fibre are related to those of its domains according to their shapes and

0022–2461

dimensions and alignments. Crack formation is one such phenomenon due to the change of domains by heat treatment.

In the present study, several mesophase pitch-based carbon fibres which show the radial properties in their transverse alignments were examined by the high resolution scanning electron microscope (HR-SEM) to elucidate the principal structural factors which induce the open crack in the transverse sections of fibres along the fibre axis. Particularly, the transverse alignment of the carbon fibre with open wedge cracks was observed in detail to form a montage of the whole area of the transverse section to clarify how the crack develops along the domains of various shape and dimension in the various alignments by further heat treatment (carbonization and graphitization).

The degree of shrinkage in the further heat-treated fibres, which is caused by the evolution of volatile materials and better stacking of aromatic layers in the micro-domains, is also discussed in relation to the domain alignment in the transverse section.

2. Experimental details

2.1. Materials and preparation of mesophase pitch-based carbon fibres

Table I summarizes some properties of mesophase pitches used in this study. Mesophase pitches (NP, mNP) were prepared from aromatic hydrocarbons, such as naphthalene and methylnaphthalene, by Mitsubishi Gas Chemical Co. using HF/BF_3 as a catalyst [13, 14]. C9 mesophase pitch (C9P) was prepared from C9 hydrocarbons by Mitsubishi Oil Co. [15] and melt-blended with methylnaphthalene derived mesophase pitch (C9/mNP = 50/50 (wt %), 320 °C, 1 h) for the preparation of the fibre with an onion skin–radial core alignment.

Naphthalene and methylnaphthalene derived mesophase pitches and their blends were spun under nitrogen pressure through a circular shaped spinning nozzle (diameter = 0.3 mm, length over diameter $(L/D) = 3$). A Y-shaped spinning nozzle was also used for the spinning fibres with random or quasi-radial transverse alignments [16]. Spinning was carried out using a mono-filament spinning apparatus [17]. Spinning conditions of the present study are detailed in Table II.

As-spun fibres were oxidatively stabilized in air at 270 °C for 20 min with a heating rate of 5 °C min^{-1} [17].

Stabilized fibres were carbonized in an argon atmosphere at 1000 °C for 10 min with a heating rate of 20 °C min^{-1}, and successively graphitized at 2500 °C for 1 min with a heating rate of 100 °C min^{-1}.

2.2. Characterization of graphitized fibres

All fibre samples were observed under a polarized light optical microscope (Olympus B061). Fibres were mounted and polished for the observation using a conventional procedure.

To examine the transverse alignments of graphitized fibres under HR-SEM (Jeol JSM 6403F), all fibre samples were cut in liquid nitrogen into approximately 0.5 cm lengths and attached to the copper grid with graphite paste. The transverse section exposed by the cutting was observed without any coating.

TABLE I Some analytical properties of mesophase pitches prepared from aromatic hydrocarbons

Code	Raw material	SP[a] (°C)	AC[b] (vol %)	Solubilities (wt %)			H/C	fa[c]	X-ray properties	
				BS	BI-PS	PI(QI)			d_{002} (nm)	$Lc(002)$ (nm)
mNP	Methylnaphthalene	205	100	52	19	33 (29)	0.69	0.81	0.3524	7.5
NP	Naphthalene	240	100	33	19	48 (31)	0.62	0.80	0.3574	3.2
C9P	C9 hydrocarbons	197	100	53	23	26	0.71	0.80	0.3512	4.2

[a] Softening point.
[b] Anisotropic contents.
[c] Carbon aromaticity.

TABLE II Spinning conditions for sample fibres

Fibre	Precursor pitch	Temperature (°C)	Pressure (kg/mm^{-2})	Amount of extrudate (mg)	Winding speed (m min^{-1})
Radial open crack	mNP	285	0.2	76 ± 2	400
Radial crack	NP	320	3.0	81 ± 3	400
Radial skin–random core	NP	315	6.0	60 ± 2	300
Quasi radial[a]	NP	325	0.8	82 ± 4	400
Onion skin–radial core	mNP/C9[b]	285	0.2	84 ± 2	400
Random[c]	mNP	295	0.1	102 ± 6	500

[a, c] Spun with Y-shaped spinning nozzle [12].
[b] Blended pitch of mNP and C9 (blending temperature: 320 °C, time: 60 min).

The height of layer stacking, $Lc(0\,0\,2)$, and the interspacing distance of layer stackings, $d_{0\,0\,2}$, of the graphitized fibres were measured according to the method defined by Gakushin (JSPS) [18], using a wide angle X-ray diffractometer (Rigaku Geigerflex; CuK_α, 0.15406 nm, 40 kV, 30 mA).

3. Results

3.1. OM observations of the transverse alignments in the graphitized fibres

Fig. 1 shows the polarized optical micrographs of sample fibres. Fig. 1a shows the optical microscopy (OM) image of the graphitized fibre with a typical radial open crack transverse alignment (F-1). Three isochromatic colour regions, blue, pink, and yellow, were definitely identified, whereas the shape and size of domains were hardly distinguished. A radial orientation of the constituent domains without 2π wedge disclinations [19] was inferred in this alignment in the OM photograph, suggesting that the radial orientation of the graphitic layers was developed from the surface to the centre of the fibre. The angle of the open crack was estimated to be around 120 degrees. However, the full identification of domain

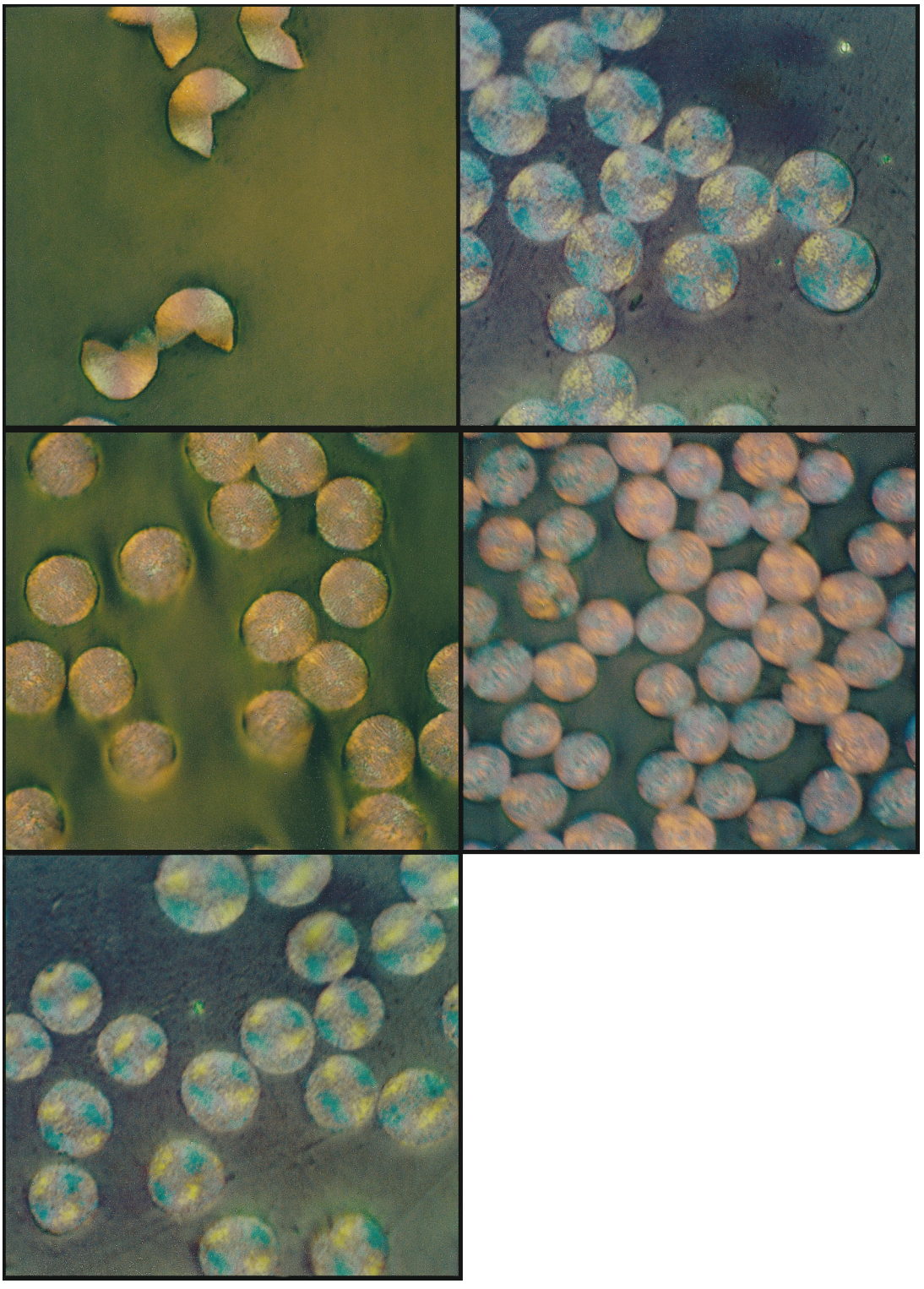

Figure 1 Reflected polarized optical micrographs in the transverse sections of the sample fibres. (a) Fibre with radial open crack. (b) Fibre with radial crack. (c) Fibre with radial skin–random core. (d) Fibre with quasi radial. (e) Fibre with onion skin–radial core.

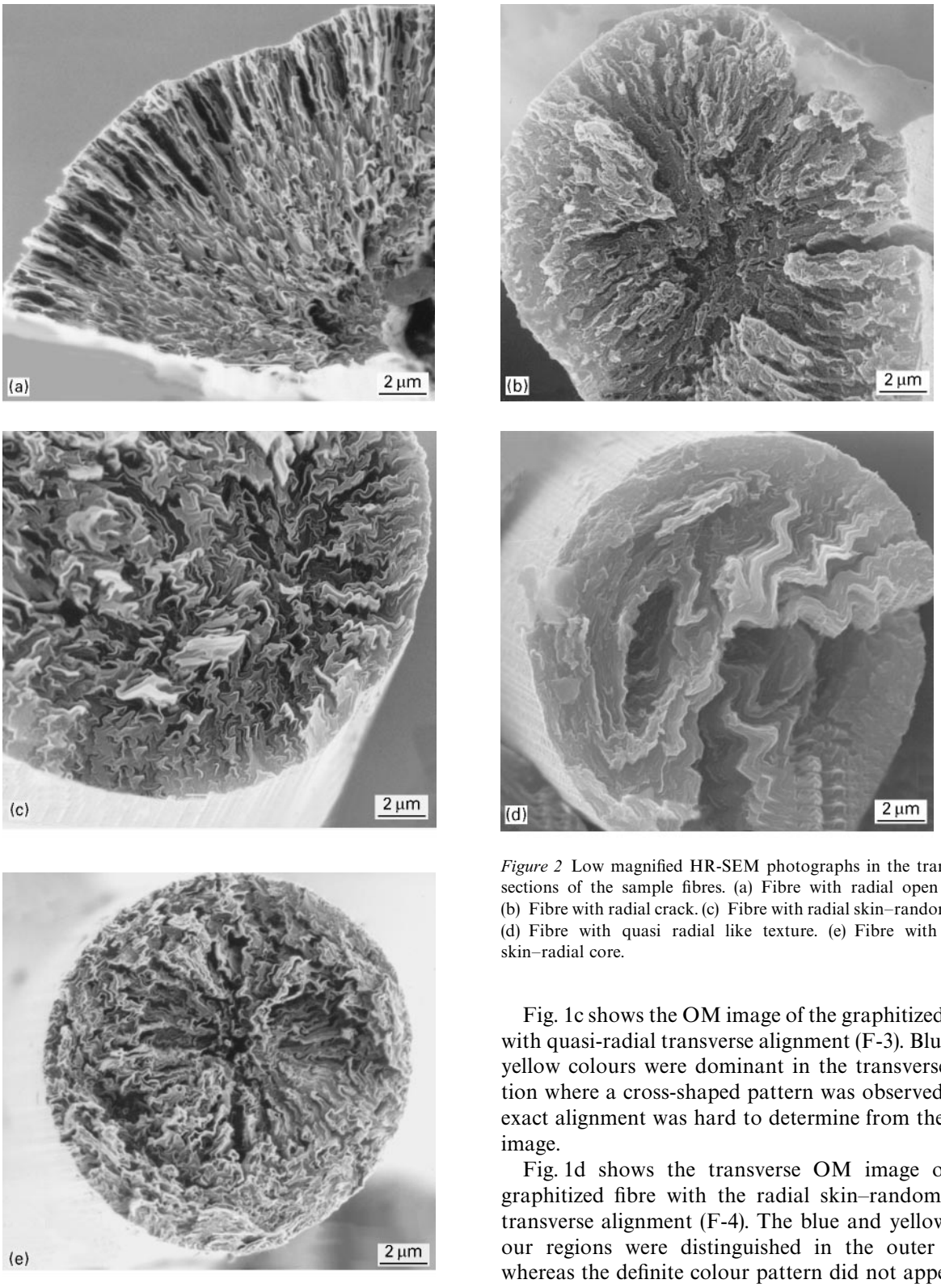

Figure 2 Low magnified HR-SEM photographs in the transverse sections of the sample fibres. (a) Fibre with radial open crack. (b) Fibre with radial crack. (c) Fibre with radial skin–random core. (d) Fibre with quasi radial like texture. (e) Fibre with onion skin–radial core.

shape, size, and distribution is still unsatisfactory with OM.

Fig. 1b shows the OM image of the graphitized fibre with a radial crack transverse alignment (F-2). Three isochromatic colour regions were also identified in the outer and intermediate parts of the transverse section, whereas the pink colour was distinguished in the centre part, suggesting non-radial alignment of the centre part. The angle of open crack was estimated to be around 10 degrees.

Fig. 1c shows the OM image of the graphitized fibre with quasi-radial transverse alignment (F-3). Blue and yellow colours were dominant in the transverse section where a cross-shaped pattern was observed. The exact alignment was hard to determine from the OM image.

Fig. 1d shows the transverse OM image of the graphitized fibre with the radial skin–random core transverse alignment (F-4). The blue and yellow colour regions were distinguished in the outer part, whereas the definite colour pattern did not appear in the intermediate and centre parts. Particularly, the mixed pattern of the blue and yellow colours, which suggested random alignment, was observed in the centre part.

Fig. 1e shows the transverse OM image of the graphitized fibre with the onion skin–radial core transverse alignment (F-5). A very special colour pattern was observed in this particular alignment. The distribution pattern of the three colours, blue, yellow and pink, was definitely distinct from those observed with the F-1 and F-2 of a radial open crack or F-4 of quasi-radial texture. The blue coloured region, which indicated the radial nature, mainly appeared in the

intermediate and centre parts, while the yellow was mainly observed in the outer part. From such a coloured pattern, unique alignment, onion skin–radial core, was defined in this fibre.

3.2. HR-SEM observations of the transverse alignments

Fig. 2 shows the low magnification HR-SEM photographs of the transverse alignments in the graphitized fibres.

HR-SEM photograph of F-1 shows that the F-1 fibre had a well developed radial domain alignment, although the outer part of around 30 nm depth from the fibre surface appeared definitely to carry a different domain alignment from that of the core area. The shapes of the constituent domains were different according to their location, gradually changing from the linear shape at the outer part into the loop one in the centre part.

Fig. 2b shows a HR-SEM photograph of F-2. The F-2 fibre carried a small crack developed in the outer part, while it exhibited approximate radial orientation in the outer part of 10–20 nm depth from the surface. No definite orientation was observable in the centre part. The shape and size of the domains were barely distinguishable at this level of magnification.

Fig. 2c shows a photograph of F-3. The approximate radial orientation was observed only in the outer area of 10 nm in depth from the surface. No definite orientation was observable in the intermediate and centre parts, with random alignment being suggested.

Fig. 2d shows a photograph of F-4. The F-4 fibre showed total radial orientation in the all transverse area. Long and multi-bent domains were aligned from the outer to the centre parts.

Fig. 2e shows a photograph of F-4. The outer part of 20–30 nm in thickness from the surface clearly showed the onion-type domain alignment, whereas the radial orientation dominated in the core part.

3.3. High magnification HR-SEM observations of the transverse sections

HR-SEM of higher magnification enables definition of the size, shapes and sub-components of each of the domains. Fig. 3 shows high magnification HR-SEM photographs of the transverse sections in the fibres, showing the radial open crack, radial skin–random core and onion skin–radial core alignments (F-1, F-3, and F-5, respectively).

The F-1 fibre showed very different domain shapes according to the location of the transverse section. In the outer part, well developed linear domains were oriented towards the centre, composed of a very

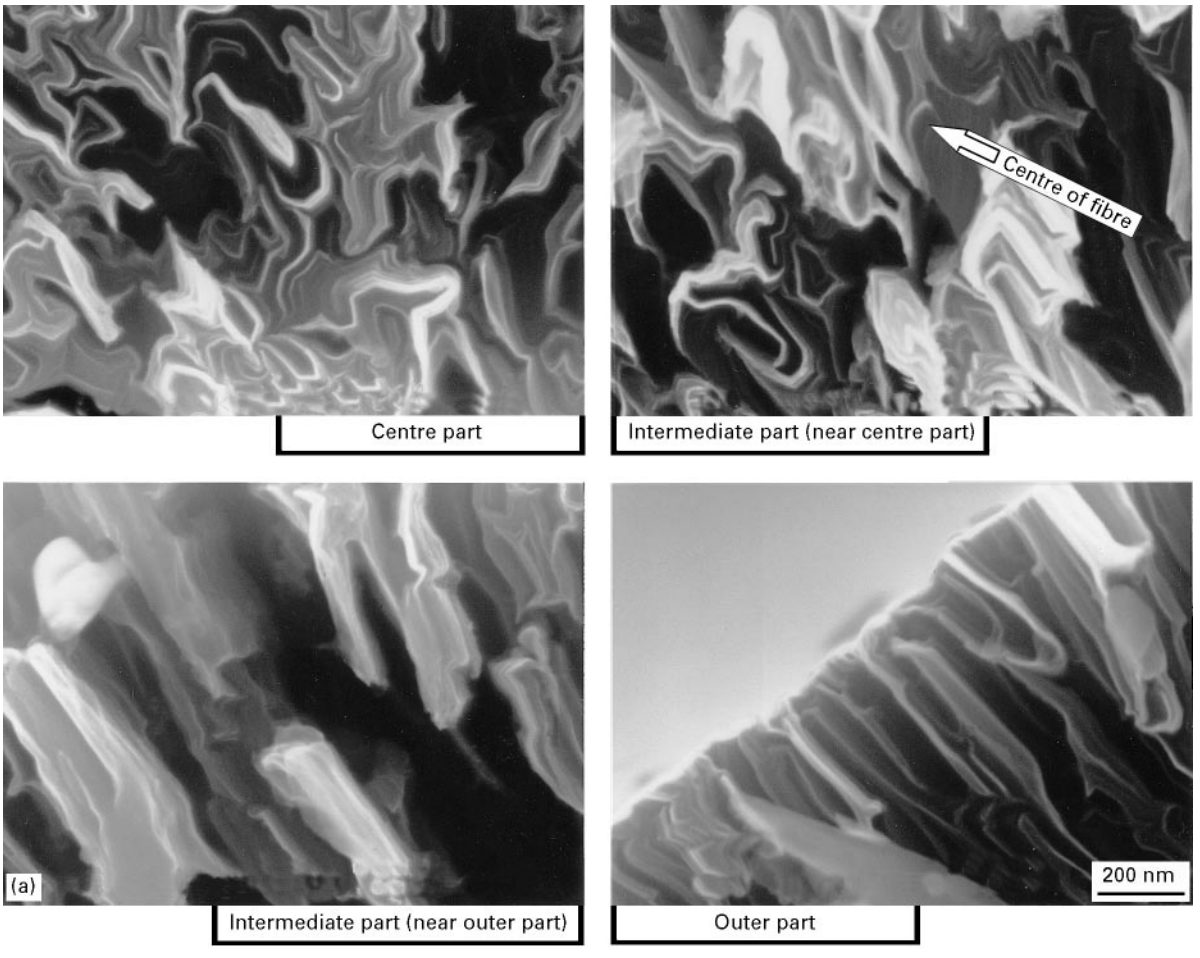

Figure 3 Higher magnified HR-SEM photographs in the transverse sections of the sample fibres. (a) Fibre with radial open crack. (b) Fibre with radial skin–random core. (c) Fibre with onion skin–radial core.

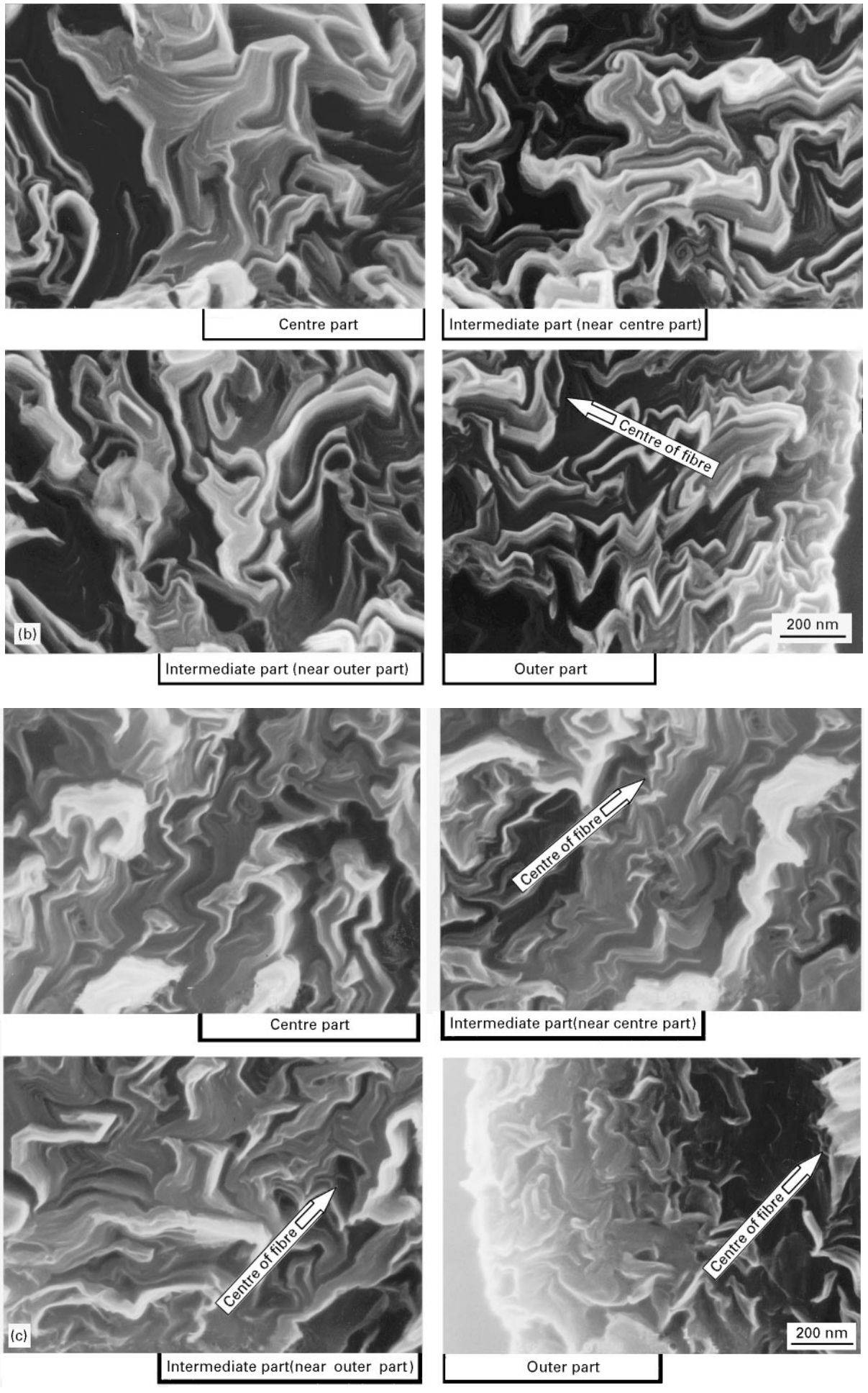

Figure 3 (Continued)

closely-packed skin area. Such linear domains gradually changed to bent or loop domains in the intermediate part even though the orientation of the domain units towards the centre was maintained. In the centre part, almost all the domains had a loop shape, distributed without any distinct alignment.

Fig. 3b shows the high magnification HR-SEM photographs of transverse sections in the F-3 fibre. The loop domains appeared almost exclusively in the whole transverse areas except for the very outer part, and were distributed in a very homogeneous manner. In the outer part, bent or multi-bent domains were observed to be approximately oriented towards the centre. No linear domain was observed in F-3.

Fig. 3c showed the photographs of transverse sections in the F-5 fibre. In the centre part, most domains had a loop or bent shape, being aligned in approximately radial orientation. In the intermediate part, almost all domains showed bent shapes, being also oriented towards the centre. In the outer part, loop or

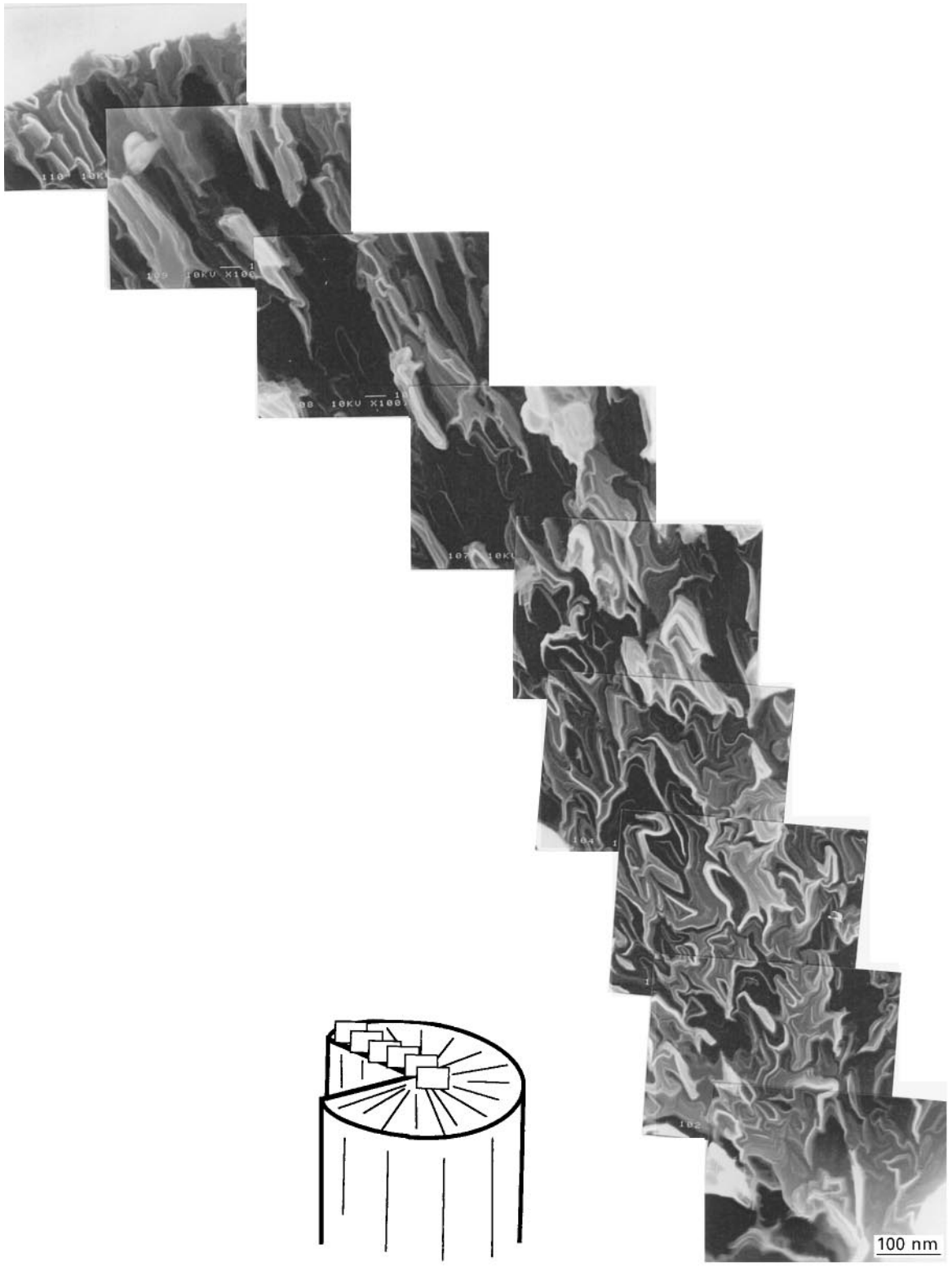

Figure 4 A montage picture of the transverse section of the fibre with radial open crack alignment.

bent domains were weakly oriented in the circumferential direction. No linear domain was found in F-5.

Fig. 4 shows a montage picture of the F-1 fibre. The montage picture clearly shows the various domain shapes according to the region in the transverse section. The linear domains spread out to 30 nm in depth from the surface. All domains in the transverse section except for those in the centre part were radially oriented, while longer units of the major loop domains in the centre part showed approximate radial orientation. Fig. 5a shows a schematic picture of domain shapes and their distribution according to transverse regions based on the montage picture of Fig. 4.

Fig. 6 shows a montage picture of the crack in the F-2 fibre. The domain shapes and some broken points were clearly seen along the wall of the shallow crack. The development of the crack appeared to be governed by the shapes and distribution of domains. Since the bent and loop domains in the intermediate and the centre parts may often prohibit crack development into the centre part, some breakage may also take place in the loop and bent domains, allowing the propagation of the crack into the centre part as confirmed in the crack wall.

Table III summarizes the principal domain shapes according to their location in the transverse sections of the sample fibres. The distribution of domain shapes in the transverse section was also estimated based on the HR-SEM images of each fibre. The fibres with cracks in their transverse section always show the linear domains with radial orientation at least in the outer part of the transverse section, although gradual change of domain shape from loop at the centre, bent at the intermediate and linear at the outer part is also observable.

3.4. Shrinkage of fibres in the heat treatment process

Table IV compares the degree of shrinkage in the diameter of the fibres showing the radial open crack and random transverse alignments. The crystallographic parameters determined using X-ray diffraction method are also summarized.

The degree of shrinkage in the fibres with the radial open crack was smaller by 6–10% than that of fibres with random alignments, indicating a preference for a circumferential shrinkage in the former fibres. The inter-spacing distance, d_{002}, of the former fibres exhibited a slightly larger value of 0.3427–0.3429 nm than that of the fibres with random alignment.

4. Discussion

The HR-SEM images of transverse sections in the mesophase pitch-based carbon fibres showing radial alignments under an optical microscope exhibited various features in alignment, dimension and domain shape, although they are approximately arranged in the radial direction. The alignment of the domains is often variable at the locations from the outer to the centre parts.

Supposing an ideal case, the linear domains may be perfectly oriented towards the centre in any location from the outer to the centre part to form perfect radial alignment in all regions of the transverse section. Such a fibre should exhibit a large open crack, of which the

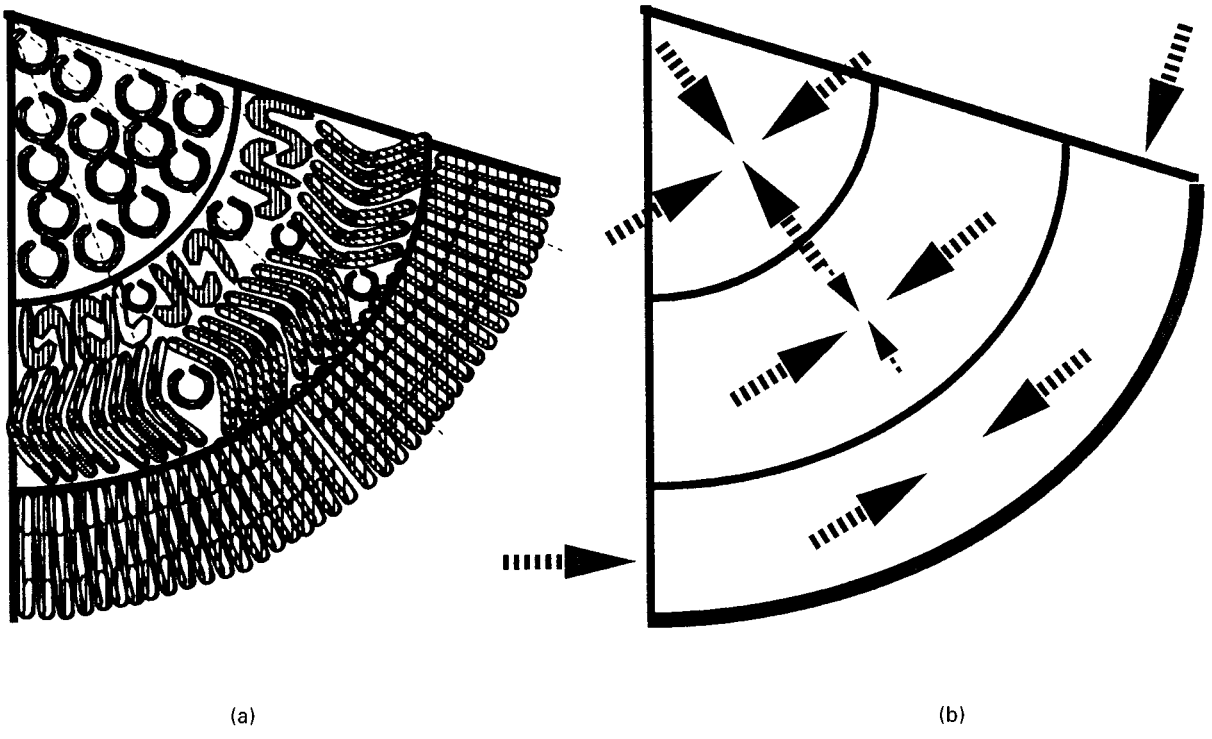

Figure 5 Schematic pictures of the distribution of domain shapes and the direction of graphitic shrinkage in the fibre with radial open crack alignment. (a) Domain shapes in the transverse section. (b) The direction of graphitic shrinkage.

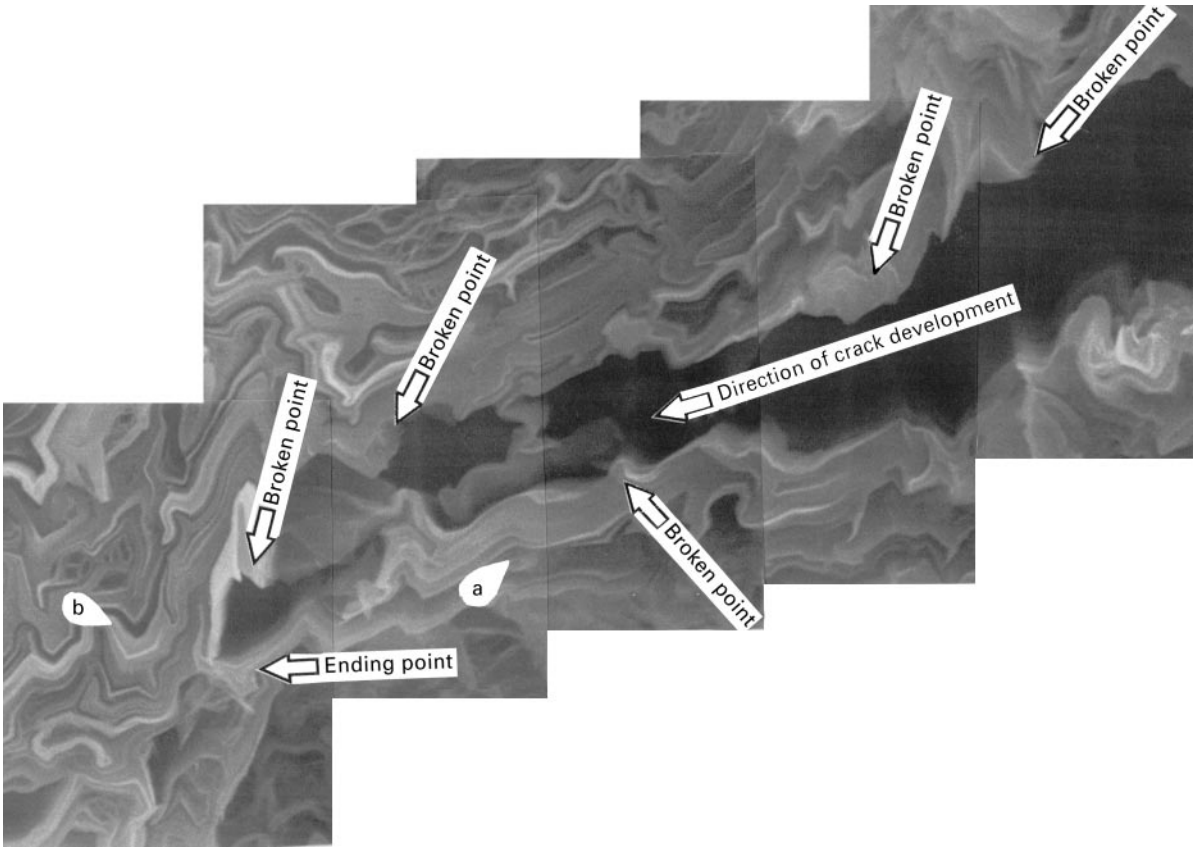

Figure 6 Shapes of domains at the crack surface: (a) bent domain, and (b) loop domain.

TABLE III Shapes and distribution of domain shapes in the transverse sections of sample fibres

Transverse alignment of sample fibre	Principal shapes of domains				Distribution of domain shapes
	Centre	Intermediate (near centre)	Intermediate (near outer)	Outer	
Radial open crack	Loop	Loop/bent	Bent/multi-bent	Linear	Inhomogeneous
Radial crack	Loop	Loop/bent	Loop/multi-bent	Linear/bent	Inhomogeneous
Radial skin–random core	Loop	Loop	Loop/bent	Bent	Inhomogeneous
Quasi radial	Loop/bent	Bent/multi-bent	Multi-bent	Multi-bent	Relatively homogeneous
Onion skin–radial core	Bent/loop	Multi-bent	Bent/loop	Loop/bent	Relatively homogeneous
Random[a]	Loop/bent	Loop/bent	Loop/bent	Loop/bent	Homogeneous

[a] Reference [2].

TABLE IV Degree of diameter shrinkage and some crystallographic parameters of fibres with radial open crack and random alignments after graphitization at 2500 °C for 20 min

Fibre	Diameter of pitch fibre (μm)	Degree of shrinkage (%)	d_{002} (nm)	$Lc(002)$ (nm)
Fibre with radial open crack alignment	21 ± 2	20 ± 1	0.3427	21
	12 ± 1	19 ± 2	0.3429	20
Fibre with random alignment	19 ± 2	30 ± 2	0.3419	23
	12 ± 1	25 ± 3	0.3422	21

angle of open crack can reach over 2π after graphitization. No crystallographic defects in the domain (disclinations or pores) should be found. So far, such a fibre has not been produced.

The linear domains form the radial alignment in the outer part, while loop ones are present in the centre part as observed in the F-1 fibre. Some loop domains often appear as schematically illustrated in Fig. 5a. In

the intermediate part of the transverse section, bent or multi-bent domains are aligned almost radially. Such an alignment allows the development of fairly large cracks which reach to the centre. It is of value to note that the wall surface of the open crack is curled at the intermediate part, following the envelope of the bent domains. Thus, an open type wedge is formed.

In the third case, linear and bent (multi-bent) domains are aligned in a rather radial manner in the outer area, producing small cracks. The very random alignment at the intermediate part stops the development of the crack into the centre, forming a shallow crack.

Non-radial alignment or non-linear domains in the outer part prohibit the development of the crack, as illustrated in the fibre with the onion skin–radial core alignment. Non-linear domains in the outer part also prohibit the development of the crack even if radial alignment is observed in the centre, as illustrated in the fibre with the radial skin–random core alignment. Random alignment of the loop domain in the outer part induces no crack. From these facts, the present authors claim that the linear domain in the outer part of the transverse section is essential for the initiation and development of cracks.

The initiation of a crack in mesophase pitch-based carbon fibres is brought about at the spinning step [20]. Molten mesophase pitch is spun into the highly oriented pitch rod through the spinning die hole and such a pitch rod is successively extended and quenched at the attenuation point to form the as-spun fibrous form. The shapes and the distribution of domains in the fibre are determined at this step. Quenching the molten pitch into the fibrous form usually induces some shrinkage by solidification. Such a volumetric shrinkage in the fibre-forming step causes the initiation of a crack if the fibre has fully developed linear domains in the outer part of the transverse section. The angle of the crack in the as-spun fibre is very small or almost zero [20]. Such an angle is broadened by the increasing heat-treatment temperature, forming a PAC-man shaped open crack in the resultant graphitized fibre [20], unless a skin–core structure is formed at the stabilization step. In this case, the role of graphitic shrinkage is merely the broadening of the open angle.

The linear domain in the outer part of the transverse section that experiences the very anisotropic graphitic shrinkage is necessary to widen the crack. The development of a crack in this case is again governed by the shapes and distribution of the domains. The bent and loop domains in the intermediate and centre parts prohibit a crack from developing into the centre region. Some breakage in the loop and bent domains confirmed the difficulty of propagating a crack into the centre part as indicated by the wall of the crack illustrated in Fig. 6.

The domain consists of micro-domains which carry several units of hexagonal carbon stacking layers, showing typically linear, bent and loop shapes as shown in Fig. 7. The graphitization allows the growth of the layers into the graphitic ones in terms of the *d*-spacing and height as well as length, bringing about

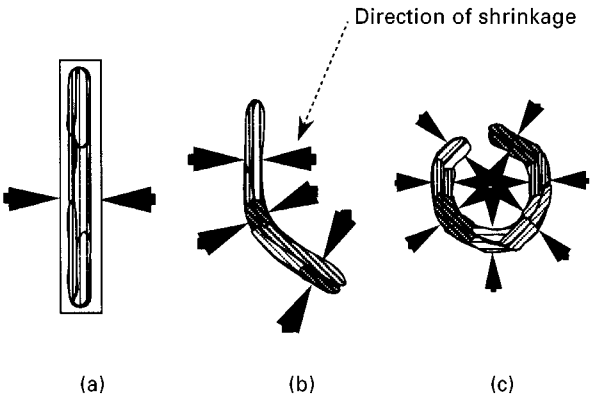

Figure 7 Typical shapes of domains and their directions of respective shrinkage: (a) linear, (b) bent, and (c) loop.

considerable shrinkage in both *a* and *c* axis directions, which is mainly associated with the evolution of volatile materials. Thus, the direction for the shrinkage of the domain is governed by its own shape or alignment of micro-domains as also illustrated in Fig. 7. The linear domain allows shrinkage to give a thinner plate. Hence, the linear domains aligned in a radial manner may allow the circumferential shrinkage to sum their respective shrinkage as shown in Fig. 5b, giving a large opened crack. The bent or loop domains may allow shrinkage in a direction dependent on their location, thereby, locally densifying themselves. Hence, if the bent or loop domains are composed of the outer part of the transverse section, the circumferential shrinkage hardly takes place.

The perpendicular alignment of the domains to the fibre wall is also observed in non-circular shaped fibres, such as tri-lobal or slit-shaped fibres. No crack development is observable in such fibres [4]. Radial or point symmetry is essential for the circumferential summation of the shrinkage [4].

When the shrinkage of respective domains takes place independently, regional cracks and voids may appear among the domains. Such a case may reduce the density of the whole fibre to give a microporous structure, causing deterioration of mechanical properties. So far the causes leading to circumferential or local shrinkage are not identified. In another case, shrinkage towards the centre of the fibre can also take place when the domains are randomly oriented, densifying the whole fibre. The latter case is desirable for better mechanical properties of the fibre.

References

1. M. MATSUMOTO, T. IWASHITA, Y. ARAI and T. TOMIOKA, *Carbon* **31** (1993) 715.
2. S. H. YOON, F. FORTIN, N. TAKANO, Y. KORAI and I. MOCHIDA, in Proceedings of International Symposium on Carbon, July, 1994, Granada, Spain (The Spanish Carbon Group, Granada, 1994) p. 682.
3. Y. YAMADA and H. HONDA, Japanese Patent Kokai 59-53713 (1984).
4. T. CHEUNG and B. RAND, in Proceedings of International Symposium on Carbon, July, 1994, Granada, Spain (The Spanish Carbon Group, Granada, 1994) p. 736.
5 T. MATSUMOTO, *Pure Appl. Chem.* **57** (1985) 1553.

6. S. H. YOON, Y. KORAI and I. MOCHIDA, *Carbon* **31** (1993) 849.
7. S. H. YOON, T. NOBUYUKI, Y. KORAI and I. MOCHIDA, in Proceedings of International Symposium on Carbon, July, 1994, Granada, Spain (The Spanish Carbon Group, Granada, 1994) p. 700.
8. K. LAFDI, S. BONNAMY and A. OBERLIN, *Carbon* **30** (1992) 569.
9. J. D. FITZGERALD, G. M. PENNOCK and G. H. TAYLOR, *ibid.* **29** (1991) 139.
10 G. M. PENNOCK, G. H. TAYLOR and J. D. FITZGERALD, *ibid.* **31** (1993) 591.
11. M. ENDO, *J. Mater. Sci.* **23** (1988) 598.
12. I. MOCHIDA, S. H. YOON, N. TAKANO, F. FORTIN, Y. KORAI and Y. YOKOGAWA, *Carbon* **34** (1996) 941.
13. I. MOCHIDA, K. SHIMIZU, Y. KORAI, H. OTSUKA, Y. SAKAI and S. FUJIYAMA, *Carbon* **28** (1990) 311.
14. Y. KORAI, M. NAKAMURA and I. MOCHIDA, *Carbon* **29** (1991) 561.
15. K. YANAGIDA, T. SAKAGI, H. YOSHIDA, K. TAKE, Preprint of 16th Annual Meeting, December, 1994. The Carbon Society of Japan, 1989, p. 38.
16. I. MOCHIDA, S. H. YOON and Y. KORAI, *J. Mater. Sci.* **28** (1993) 2331.
17. F. FORTIN, S. H. YOON, Y. KORAI and I. MOCHIDA, *Carbon*, in press.
18. JAPAN SOCIETY FOR PROMOTION OF SCIENCE (JSPS), *TANSO* **36** (1963) 25 (in Japanese).
19. C. B. NG, G. W. HENDERSON, M. BUECHLER and J. L. WHITE, in Extended Abstracts of Biennial Conference on Carbon, San Diego, California, 1983, p. 515.
20. N. TAKANO, S. H. YOON, Y. KORAI and I. MOCHIDA, *Carbon*, to be submitted.

Received 12 October 1994
and accepted 13 February 1996